DOI: 10.1002/admi.201700875
Article Type: Full Paper

Rapid formation of Macroscopic Self-Assembly of Liquid Crystalline, High Mobility, Semi-conducting Thienothiophene

Manish Pandey, Ashwathanarayana Gowda, Shuichi Nagamatsu, Sandeep Kumar, Wataru Takashima, Shuzi Hayase and Shyam S. Pandey**

Dr. M. Pandey, Prof. W. Takashima, Prof. S. S. Pandey, Prof. S. Hayase
Graduate School of Life Science and Systems Engineering
Kyushu Institute of Technology
Wakamatsu, Kitakyushu, 808-0196 Japan

A. Gowda, Prof. S. Kumar
Soft Condensed Matter Group
Raman Research Institute
C. V. Raman Avenue, Sadashivnagar, Bangalore, 560080 India

Prof. S. Nagamatsu
Department of Computer Science and Electronics
Kyushu Institute of Technology
Iizuka, 820-2502 Japan

Keywords: Self-assembly, Orientation, Thienothiophene, Anisotropic-transport, OFET

A synergistic approach of enhancing the charge carrier transport in organic semiconductors along with the facile solution processing while maintaining the high performance is undoubtedly crucial for the proliferartion of organic electronics. Floating film transfer method (FTM) has been used as a facile and highly cost-effective method for the fabrication of large scale uniform and highly oriented films of poly[2,5-bis(3-tetradecylthiophen-2-yl)thieno[3,2-b]thiophene] (pBTTT C-14) under ambient conditions. Utilization of such oriented films as an active semiconducting layer in organic field transistors (OFETs), conspicuously exhibited highly anisotropic charge carrier transport. The highly oriented FTM processed thin films of pBTTT C-14 have been well characterized by polarized electronic absorption and Raman

spectroscopy, atomic force microscopy, out-of-plane X-ray diffraction along with the grazing incident X-ray diffraction (GIXD) measurements. A perusal of the GIXD results have clearly corroborated an edge-on orientation with complete absence of face-on oriented counterparts which is highly desired planer devices like OFETs. Utilization of these oriented films for OFETs led to about 10 times of mobility anisotropy and highest mobility measured along the backbone orienation direction has been found to 1.24 $cm^2.V^{-1}.s^{-1}$ which is one of the highest amongst repported values for this class of materials under similar device configurations.

1. Introduction

Organic semiconductors have attracted immense attentions of the scientific community owing to their tremndous technological potential in the area of organic field effect transistors (OFET), light emitting diodes, solar cells [1]. It can be envisioned that carrier mobility exceeding the benchmark of amorphous silicon (~1 $cm^2V^{-1}s^{-1}$) is enough for the practical applications in order to minimize cost of production.[1,2] A number reports on molecular semiconductors giving consistently higher mobilities (> 0.1 $cm^2V^{-1}s^{-1}$) although exist but their application to large area flexible substrates while maintaining the silimar morphology is still cumbersome. Recent researches on the serach for high performance organic semicondcutors have witness that majority of them exhibit the high performance when vacuum deposited or growing single crystals due to their highly rigid nature which in-turn limits their application potentials especially towards the realization flexible electronic devices.[3,4] In this context, semiconducting conjugated polymers (CPs) seems to be a viable alternative due to their facile solution processability, flexibility and tailor-made synthetic versatility.[5] However, molecular self-assembly driven and morphology dependent device performance makes this a critical issue for the judicious selection of suitable thin film fabrication technique.[6–8] Charge transport in CPs are essentially comprised of intramolecular

(with in conjugated backbone), intermolecular through π-π stacking of the adjacent stacked conjugated backbones, and finally intermolecular inter-domain hopping.[9]

Molecular self-assembly is the obvious tendenacy of CPs by the virtue of their inherent one-dimensionality planar molecular structure owing to extended π-conjugation. Therefore, unidirectional orientation of CPs can be considered as one of amicable way not only to impart the facile carrier transport but also to understand the anisotropic charge transport behavior.[10,11] In the OFETs based on thin films of oriented CPs, where the charge transport takes place at the semiconductor-insulator interface highly depends on the processing methods adopted for thin film fabrication. Looking towards the three dimensional arrangements of macromolecules of the CPs in the cryatalline domains, lamellar (a-axis), π-π stacking (b-axis) and conjugated backbone (c-axis), high in-plane carrier transport is expected in the bc-plane parallel to the surface (edge-on orientation).[12] It has been widely accepted that this edge-on orientation of CPs is thermodynamically more favorable for in-plane carrier transport which can be easily achieved by controlled and slow film growth and critically influences the field-effect mobility.[13,14] Recent past has witnessed the implimentation of various methods such as friction transfer, mechanical rubbing and strain alignment for imparting the long range ordering of the polymers.[15–18] Although shear force assisted friction transfer and mechanical rubbing seems to be suitable for realizing molecular ordering but are unable to provide edge-on orientation as well as thickness control along with maintaing the orientation. [15,17] On the other hand, strain alignment is applicable for the films with high ductility and quite often leads to cracking in the films especially using highly crystalline CPs limiting the versatility of this method.[18–20] Therefore, development of a facile method capable of forming highly edge-on oriented uniform films while preserving the orienation along with the thickness control is highly desirable. We have developed an interesting floating film transfer method (FTM) for the facile and large sacle fabrication of oriented films of CPs

which utilizes the formation of floating films of CPs on a hydrophilic liquids substrates with natural evaporation hydrophobic solvent.[21] This method could considered as simplified version of Langmuir Blodgett (LB) technique where there is no application of external surface pressure and viscosity of the hydrophilic liquid substrate solve this purpose to orient the CPs. Moreover, FTM is capable of forming multilayer thin films to control the desired film thickness while preserving the orientation.[21,22] Films of CPs fabriacted by FTM offers various advantages over most commonly employed spin-coating not only in terms of device performance but also easiness for attaining the macroscopic orientation by parametric optimization of the casting conditions.[23]

Amongst various thiophene based CPs, poly[2,5-bis(3-tetradecylthiophen-2-yl)thieno[3,2-b]thiophene] (pBTTT C-14) is one of the most studied semi-crystalline CP owing to its significantly high carrier transport and device performance based on this material.[2,5,24] Recent researches have clearly indicated that increasment in charge transport of the pBTTT was demanstrated by increasing the ordering between their poymeric backbones leading to the reduced inter-chain and intra-chain resistance with enhanced π-π stacking. A perusal of the majority of research works done on the pertaining to the molecular ordering of pBTTT in order to improve the charge transport reveals the utlization of the shear forces at an elevated temperatures near to their liquid crystalline mesophase.[19,25,26] Another bottleneck of pBTTT is its poor solubility in the common halogentated organic solvents at room temperature. This the reason for the lack of reports neither regarding self-aseembly on templates nor time-dependent supramolecular fiber formation for this material unlikly to other thiophene and fluorene based CPs.[27–31] In this paper, we have demonstrated the macoscopic orientation of the pBTTT through our newly developed FTM. Utilization of FTM has led to the fabrication of large scale uni-axially oriented uniform thin films under ambient condition without using any sophisticated instrument and its transfer to any desired substrates for characterization and application. To the best of our knowledge, the orientation intensity and

crystallinity exhibited by these films is the highest amongst the values reported for pBTTT with well defined edge-on oriented crytallites. Application of these highly oriented films for OFET fabrication with bottom gated top contact geometry, a saturation field effect mobility reaching 1.24 $cm^2V^{-1}s^{-1}$ was obtained representing the highest value of mobility amongst reported values with similar device configurations. Film morphology of the oriented films were characterized by polarized absorption spectroscopy, polarized Raman spectroscopy, Atomic force microscopy (AFM) and out-of-plane X-ray diffraction (XRD) and in-plane grazing incident X-ray diffraction (GIXD) measurements.

2. Results and Discussion

Unlikely to other polythiophenes such as poly(3-hexylthiophene) P3HT, Poly(3,3'''-didodecyl-quarterthiophene) (PQT-C12), the low solubility of pBTTT is associated with the very strong π-π interactions between the chains of pBTTT macromolecules. To provide good solution processability it is necessary to heat the polymer solution at relatively higher temperatures (>80 °C) which compells to choose the solvent with higher boiling point. This is the reason why chlorobenezene or 1,2-dichlobenezene have been widely used for solution based thin film fabrication of pBTTT by spin coating, doctor blading, flow coating, and zone-casting in the recent past [24,25,32]. Utilization of these methods in combination with high boiling solvents and slow solvent evaporation imparts sufficient time for the self-organization of the polymeric chains leading to the thermodynamic stable edge-on orientation [13,14].

2.1. Fabrication of Macroscopically Oriented pBTTT Films by FTM

It has been previously reported by our group that FTM provide large scale oriented films of the CPs and extent of molecular orientation depends on subtle control on film casting parameters like viscosity, temperature of liquid substrate, concentration of polymer solution and nature of polymeric backbone.[23] Unlikely to LB film preparation where there is a need of amphiphilic molecules and film compression to align the molcules on air/water interface

while in FTM, formation of floating film and indcution of molecular orienation is simultaneous.[22,33] It was also found by us that CPs exhibiting inherent liquid crystalline behavior have tendency of molecular orientation by FTM and film formation takes place by lyotropic phase assisted self-assembly during the rapid solvent evaporation and solidification.[34] In this work, pBTTT has been selected as organic semiconductor for fabricating the OFET where FTM has been use to prepare the oriented thin film of this CP. Owing to the poor solubility this polymer at room temperature, it was dissolved in the hot chloroform and a small amount (~15 μl) of this solution was dropped in the center of the petri-dish (radius = 7.5 cm) containing the viscos liquid substrate consisted of a mixture of ethylene glycol (EG) and glycerol (GL) (3:1). The polymer solution undergoes rapid spreading in all of the direction over the entire size of the petri-dish as shown schematically in the **Figure 1**a,b (for details please see the supporting video). Fabrication of oriented thin films in the FTM has been schematically shown in the Figure 1c. Application of the hydrophobic polymer solution on the viscous hydrophilic liquid substrate leads to fast expansion of the polymer solution followed by solvent evapaoration leading to the formation of the floating film.

Inherent liquid crystallanity (LC) of pBTTT assist the molecular self-assembly in the propagating film while viscosity of the liquid susbtrate poses a dragging force to this propagating floating film during the spreading resulting in to macorscopically oriented films as schematically shown in Figure 1c. Orientation in this film fabricated by FTM was easily visible using a polarizer film only by rotating it in parelled and perpendicuolar to the film propagation direction. Nature of orienations in CPs like edge-on or face-on play a crucial role in controlling the device performance. An edge-on orientation is preferred for planer devices like OFETs while face-on orientation is highly desired for vertical devices like solar cells or light emitting diodes. We have also reported the attainment of edge-on as preferred

orientation in non-regioconrrolled poly(3-hexylthiophene) prepared by FTM. [22,33] In the case of pBTTT films prepared by FTM, polymer itself is highly hydrophobic owing to its very long alkyl chain (tetradecyl) and fabrication of film is condcuted on highly hydrophilic viscous liquid substarte with multiple –OH groups (EG and GL). The obvious inherent repulsion between the the –OH groups of hydrophilic liquid sustrate and hydrophobic alkyl group of pBTTT. At the same time, lack of hydrogen bonding with S-atom of thiophene ring in the polymer and –OH group of liquid substrate denies the possibility of any face-on orienation and promote the thermodyanamiucally stable edge-on orienation as schematically shown in the Figure 1c.

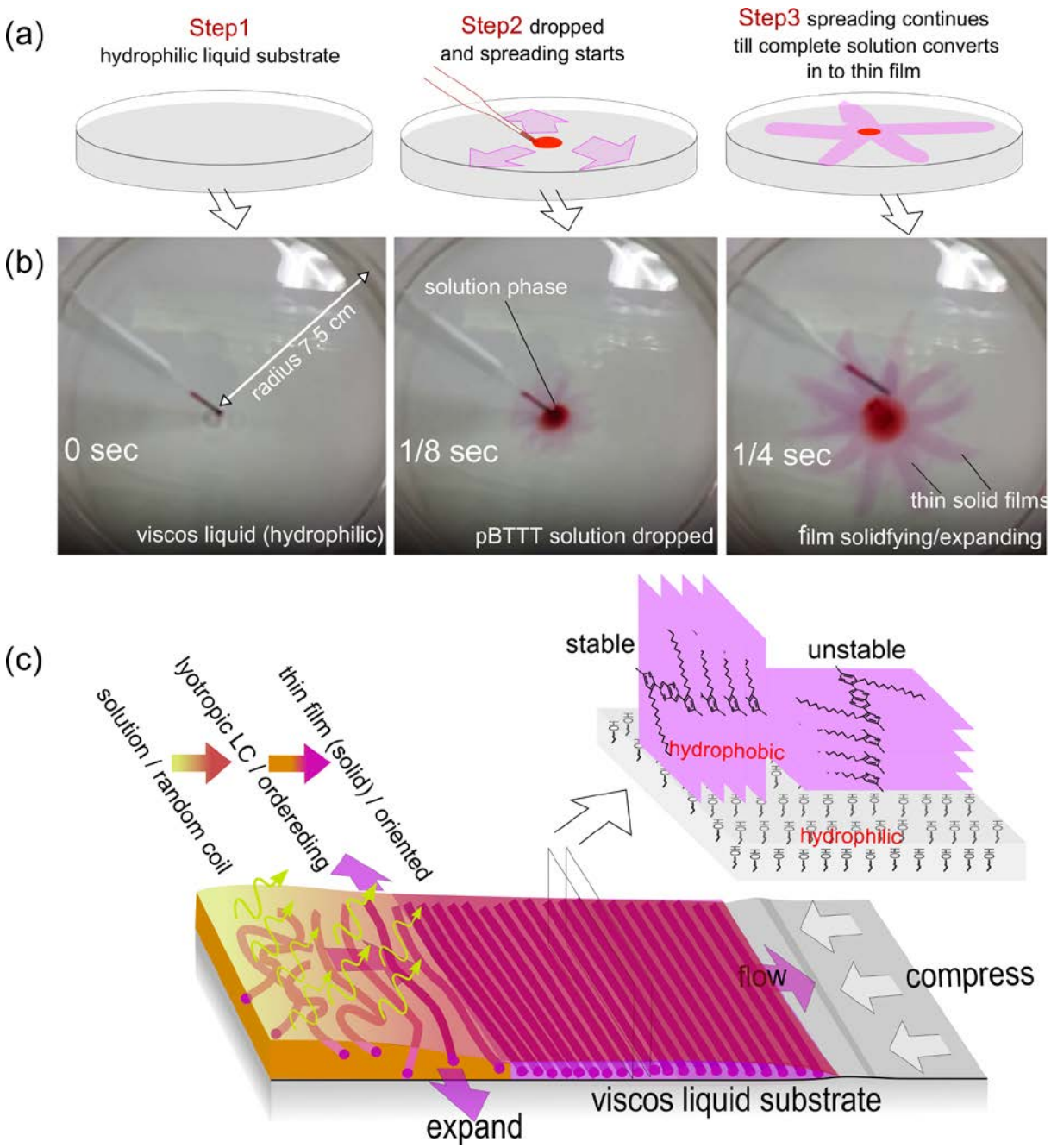

Figure 1. Schematic Illustration of the steps (a) and photographs (b) of the processes occuring while film formation, (c) Schematic representation of the possible mechanism for orientation during the film formation of pBTTT on liquid substrate.

2.2. Characterization of Oriented pBTTT C-14 Films

Owing to the large scale and uniaxial orientation, the orientation behavior of these films can be easily monitored by naked eye using a linearly polarized film. **Figure. 2**a, depicts the optical photographs of the FTM frocessed thin film of pBTTT on glass along with the visual perception of macroscopically orientated film simply by rotating the polarizer film.

When these films were further subjected to the polarized optical microscopy (POM), it shows intense color change from dark to light when polarization angle of the incident light was changed from orientation direction 00° to perpendicular 90° as shown in Figure 2b. Quantitative analysis of the molecular alignment of pBTTT was characterized by polarized electronic absorption spectra the films. Since the pBTTT is well known to give thermotropic LC behavior between 120°C-130°C (terrace phase) as measured by differential scanning calorimetry (supporting information Figure S1).[25,32] Polarized absorption spectra for the both of the as-cast and annealed films are shown in Figure 2c. In oriented film, polarized light interact maximum when parallel (||) to the orientation direction giving maximum absorbance and vice-versa in the perpendicular ($\perp$) direction. This optical anisotropy of the orineted film can be quantified by dichroic ratio (DR), which is defined as $DR = A_{\parallel}/A_{\perp}$, where $A_{\parallel}$ and $A_{\perp}$ are the maximum absorbance in parallel and perpendicular directions, respectively. The measured DR was found to be 3.2 in the as-cast films and increases drastically to >10 reaching up to 13 upon annealing the films for 2 mins above its mesophase temperature (180 °C). As compared to the parallel absorption spectra of the films, a clear blue-shift can be seen in perpendicular spectra which represents the presence of randomly distributed macromolecules with relatively lower molecular weight fractions.[35] Uniqueness of the FTM lies in the isolation formation of solid oriented film on liquid substrate and then transfer of the film on any desired substrate for further charaterization and applications. Therefore, a pertinent question arises about the idientification precise direction of orientation and keeping this in mind, angle dependent absorbance was also maesured and results are shown in the Figure 2d. The value of absorption maximum (λ_{max}) was found to be in spreading direction (00°) and tends to decrease in both of the sides while rotating the substrate in anti-clockwise (-90°) and clockwise (+90°) during film transfer. This suggetss that there is the least possiblity error occuring during film casting on any substrate owing to the high macroscopic

orientation of polymer backbones. To the best of our knowledge, this orientation intensity values are the highest till date for pBTTT C-14 for both in as cast as well as annealed.[19,25,36,37] Previously high orientation has only been achieved in the analogous of thienothiophene polymers (pBTTT C-12 and C-16), when the casted films were subjected to mechanical rubbing and film compression on ionic liquids. Moreover these orientation processes reported for pBTTT were carried at elevated temperature near their LC phase transition temperatures and extent of orientation was reported to be low below 100°C. [26,37]

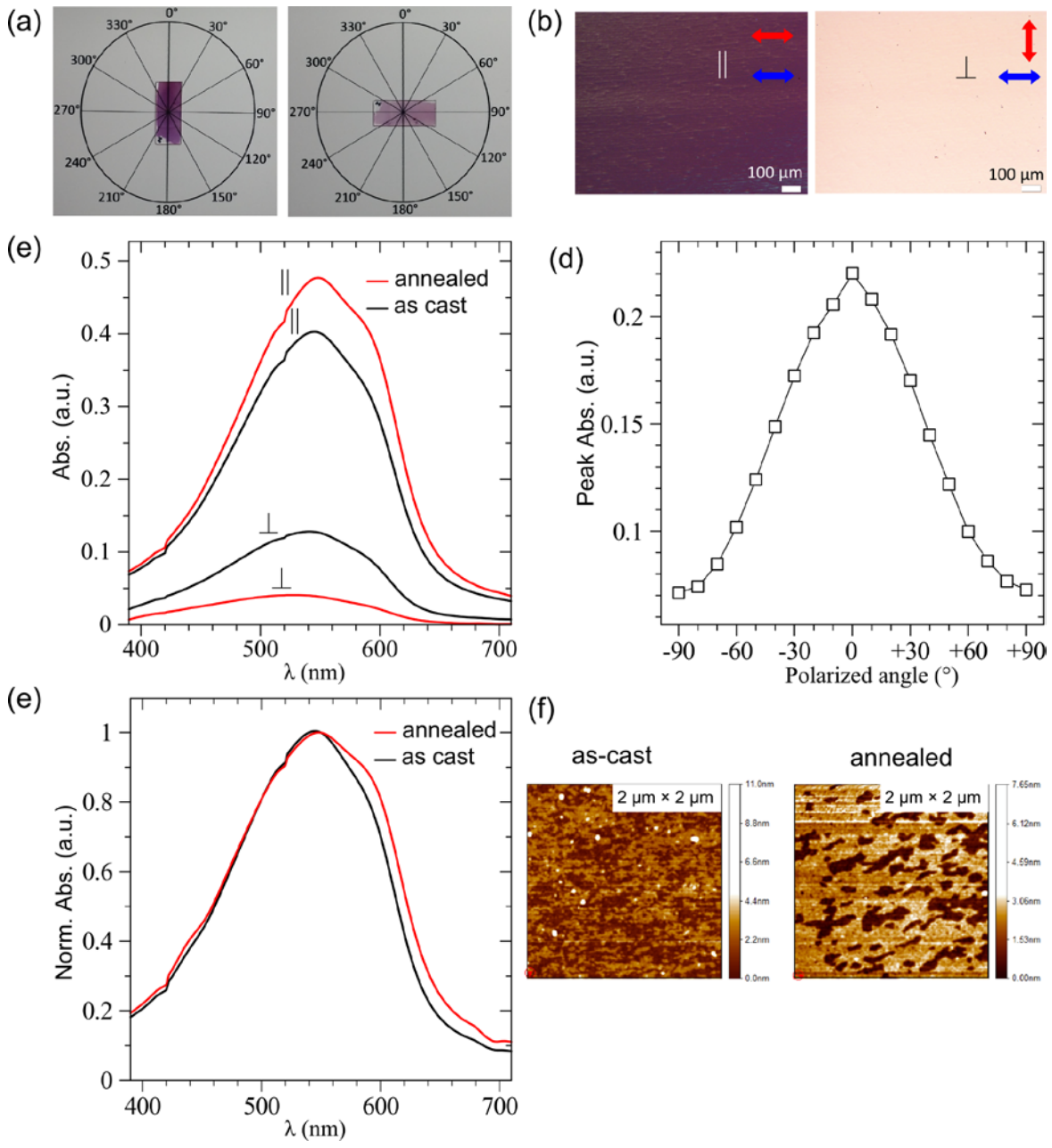

Figure 2. Optical photograph (with linear polarizer) (a) and corresponding polarized optical microscopic images (b) of as oriented film on glass substrate at 0° (||) and 90° (⊥) , (c) Polarized electronic absorption spectra of the as-cast and annealed film, (d) Angle dependence of peak absorption of as-cast oriented film, (e) Normalized absorption spectra of as-cast and annealed film, (e) AFM topography of the as-cast and annealed films on OTS treated SiO_2 substrates. The double sided red and blue arrow in (b) represents the polarization direction of incident light and orientation direction of pBTTT, respectively. 0° and 90° are tangential and parallel to the film expansion direction from the center/drop point of the polymer solution on liquid substrate.

Normalized electronic absorption spectra of FTM processed thin films of pBTTT shown in the Figure 2 (e), exhibited λ_{max} at 544 nm and 548 nm for as-cast and annealed films, respectively. This slight bathochromic shift upon annealing of the film indicates the increase in the effective conjugation length while pronounced vibronic shoulder further supports the high degree of ordering and improved π-orbital delocalization due to terrace phase formation after annealing.[25,38] Figure 2 (f) shows the formation of large terrace phase domains extending upto several hundreds of nanomenters upon annealling of the the as-cast films which is in well aggrement with previous reports.[39,40] Futhermore, these oriented film posses high uniformity upto cm scale as probed by two dimensional positional mapping of peak absorption (supporting information Figure S2).

To have the further in-depth understanding of orientation characteristics of pBTTT c-14 in both of the as-cast and annealed films, polarized Raman spectroscopic investigations were also carried out. **Figure 3** depicts polarized Raman spectra while correspondig major Raman bands of the polymeric backbone are listed in the **Table 1**.[41] In the case of polymer backbones lying along the orientation direction and uni-axially polarized beam was in parallel to the orientation direction, it will encounter with the majority of the C–C and C=C bonds resulting in to enhanced signal intesity.[34,42]

Table 1. Typical Raman peaks assignments of pBTTT c-14

peak	frequency (cm^{-1})	assignment[a]
ν_1	1391	thiophene C–C
ν_2	1415	thienothiophene C=C stretch
ν_2	1467	Inter-ring C–C stretch
ν_3	1489	thiophene C=C stretch

[a]Peak assignment as determined by the DFT simulation in ref .[41]

A perusal of Figure 3 pertaining to the Raman spectra for both of the as-cast and annealed films clearly corroborates that intensity of the charcaterstic Raman bands lying along the pBTTT conjugated backbones decreases while moving the beam from 00° to 90°. The obvious higher intensities as well as the differences in the annealed films were found after the annealing, which arises from the high degree of ordering with large domains as discussed above. It can be clearly seen that intensities of Raman band associated with the C=C bond of thiophene and thienothiophene ring stretching are relatively more sharp with decreased full-width half-maximum (FWHM) along the orientation direction representing the high degree of π-electron delocalization. On the other hand there was no peak shift in the Raman bands of the characteristic bonds upon changing the orientation from parellel to perpendicular. It is worth to mention here that unlikely to pBTTT in present case, anisotropic poly(3-hexylthiophene) (P3HT) exhibits a significant decrease in the frequency corresponding to C=C bond stretching.[34,42] Exact reason for this behavior pertainiling to this absence of any peak shift in pBTTT is not known clearly but it might to be associated with the rigid-rod like behavior of pBTTT, since vibronic position of pBTTT also do not show aprreciable changes upon orientation. [25,43,44] Contrary to this, P3HT is well known to exhibit significant changes in electronic absorption spectral features like absorption maximum, FWHM and vibronic

shoulders etc for different kind supramolecular assemblies as well as orientation behavior as discussed previously by many researchers.[8,35,38,44]

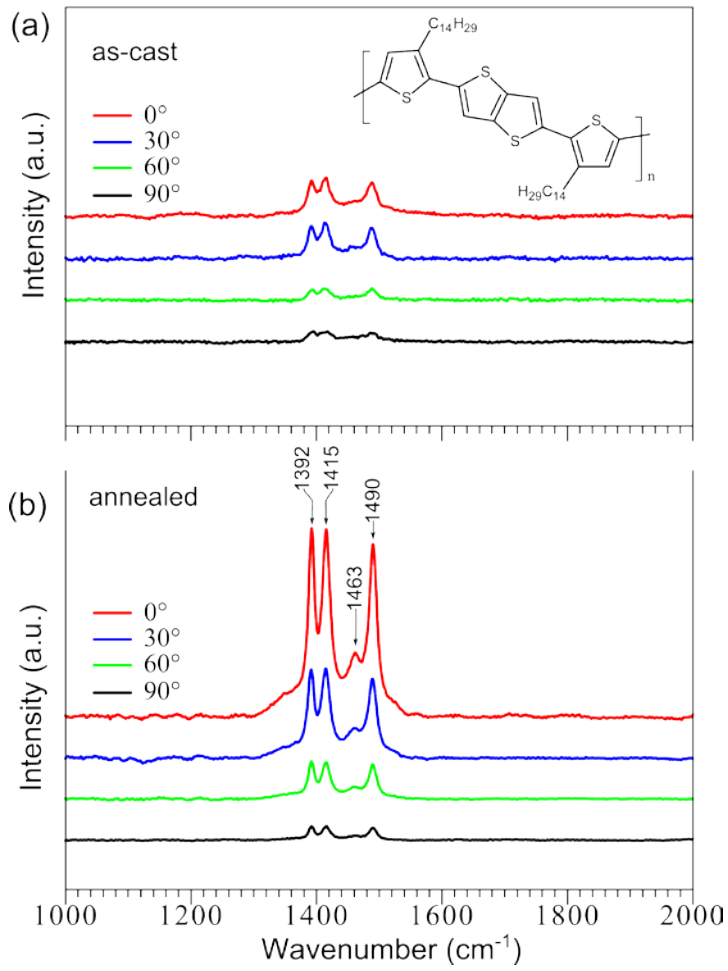

Figure 3. Polarized Raman spectra of oriented pBTTT films (a) As-cast and (b) annealed at 180°C. All the characteristics peaks were found to be intense when the backbone was parallel (0°) to beam direction, which decreases while rotating the direction of incident beam towards (90°). The inset in the (a) shows the chemical structure of the pBTTT C-14.

In order to investigate the film crystallinity and stacking of domains in the oriented films prepared by FTM, XRD measurements were also carried out in both of the out-of-plane and in-plane at grazing angle. Same films have been utilized for the measurents before and after annealing in order to avoid any kind of differences arising from the sample to sample variations. **Figure 4**a shows the out-of-plane XRD patterns for as-cast (oriented floating film) as well as annealed films. A strong series of (h00) peaks up to 3rd order related to a-axis were

observed in the oriented films which becomes more prominant up to 4th order after thermal annealing. In order to compare isotropic films with similar thickness were also prepared by spin-coating as shown in Figure 4b. In spite of the obvious similar trend, it can be clearly seen that all the peaks corresponding to the lamella formation by alkyl side-chain stacking in the FTM films were more pronounced up to higher order as compared to the spin-coated films. By looking at diffraction pattern of both oriented and spin-coated films, it can be easily interpreted that these oriented films exhibits high level of crystallinity as compared to that of the spin-coated films in both of the as-cast as well after thermal annealing. The details of these peaks pertaing to the out-of-plane diffraction are listed in the **Table 2**.

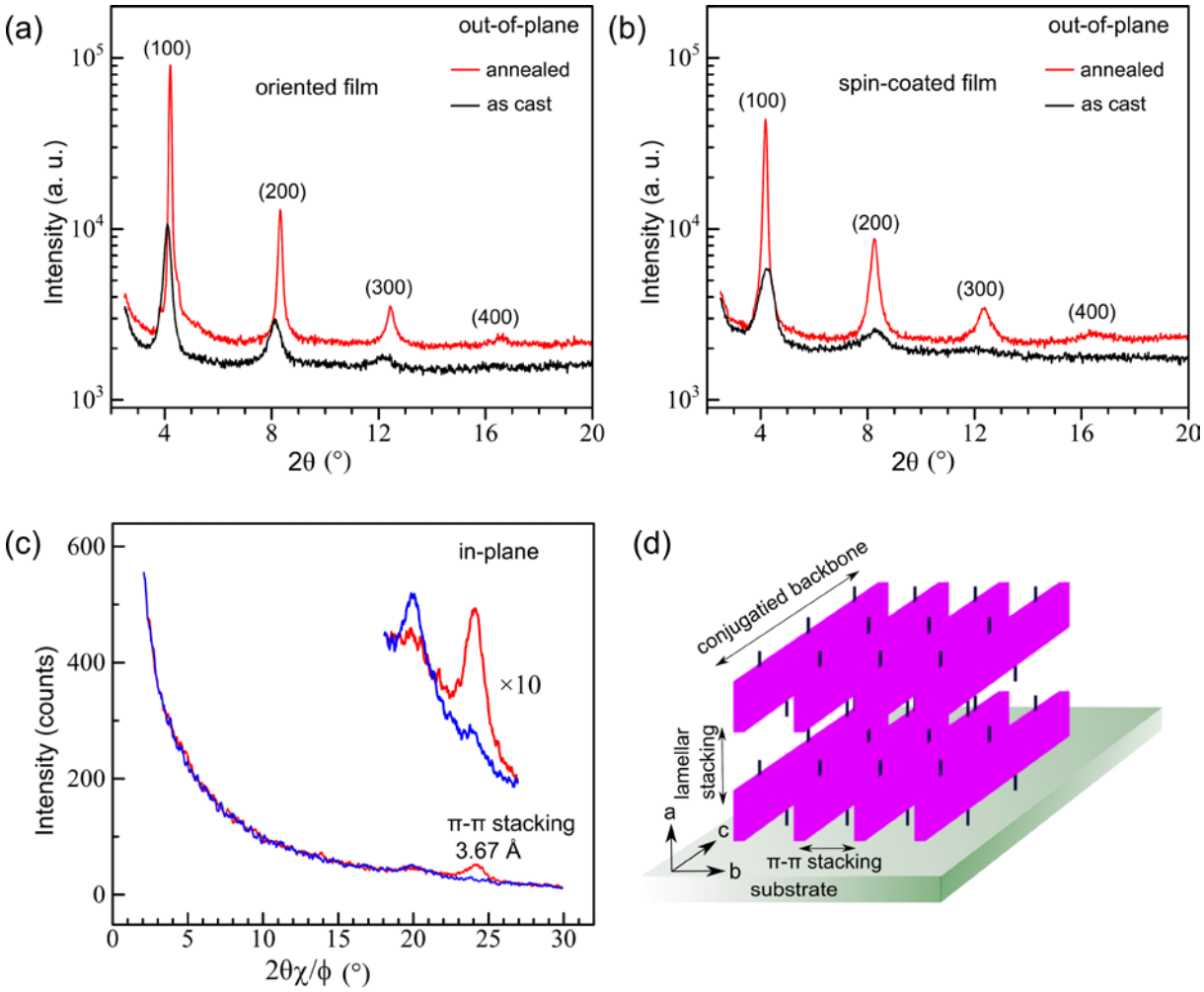

Figure 4. Out-of-plane XRD patterns of oriented (a) and spin coated (b) pBTTT films. In-plane GIXD of oriented pBTTT film (c) and schematic representation of the orientation of pBTTT macromolecules with respect to the substrate. The red and blue line in 2θχ/ϕ patterns of in-plane GIXD patterns depicts scattering vector to be perpendicular (red) and and parallel (blue) to the orientation direction.

The *d*-spacing along the a-axis in the oriented as-casted and annealed films were found to be 21.5 Å (2θ = 4.1°) and 21 Å (2θ = 4.2°), respectively (Table 2**)**. In general, position of the peak represents the distance of lamella stacking related to the interdigitated alkyl side-chains whereas sharpness of the peak is associated with the crystallinity and grain size.[39,45,46] A little higher *d*-spacing in the as-cast films might be associated with the stretching of the alkyl side chains while the film formation on the hydrophilic liquid by FTM. It was found to be decreased upon annealing due to increased inter-digitation by rearrangement of the alkyl side chains while recrystallization of the melted side chains.[45] It is also worth to note that such differences in distances between the lamella planes is not observed in the spin-coated films, which clarify that the no siginificant changes in inter-digitation takes place before and after annealing. Oriented films prepared by FTM exhibits relatively intense as well as sharp peaks (reduced FWHM) which is attributed to the enhanced film crystallinity which are clearly visible in the Figure 4 (a,b) and Table 2. Oriented films in this work are considerably sharp while FWHM is limited by the incident X-ray resolution but comparable to highly crystalline films of pBTTT studied by synchrotron sources.[39]

In-plane GIXD measurements were also carried out for the as-cast oriented films in order to the investigate orientation characterstics more precisely. It can be seen in figure 4c that when the incident X-ray was parallel to the backbone direction, there was a clear peak at 2θ = 24.2° corresponding to the face-spacing between the main-chain of pBTTT representing π-π stacking distance which was found to be 3.67 Å similar to reported values.[37] On the other hand, when incident X-ray was perpendicular to orientation direction, only repeated unit peak was found with no π-π stacking peak. Complete absence of the series of peaks related to the lamella stacking of the alkyl side-chains also represents that these films were only edge-on oriented with backbone and π-π stacking lying in plane of the substrate, which is considered to be the best spatial orientation of the crystallite to have high in-plane transport.[47] The in-

plane GIXD clearly indicates that the main chains of pBTTT were aligned uni-directionally perpendicular to spreading direction of the floating film.

Table 2. Characteristics of out-of-plane X-ray diffration peaks of as-casted and annealed oriented and spin coated films, respectively.

Film/Annealing Condition	Peak Index	2θ (°)	FWHM (rad)
oriented Film	(100)	4.10	0.0046
	(200)	8.12	0.008
annealed at 180°C	(100)	4.20	0.0016
	(200)	8.3	0.0027
as-spun	(100)	4.23	0.010
	(200)	8.31	0.016
annealed at 180°C	(100)	4.18	0.0033
	(200)	8.25	0.0052

2.3 Charge Transport Anisotropy in Oriented pBTTT C-14

In order to estimate the impact of these highly oriented films on the in-plane charge transport properties OFETs were fabricated in the bottom gate top contact geometry as shown in **Figure 5**a. In order to compare the charge transport capability in the direction of backbone orientation and π-π stacking, the channel direction was varied with respect to the orientation at different intervals of 30° from 0° (||) to 90° (⊥). Figure 5b,c shows the typical OFET characteristics (output and transfer curves) of OFETs. There was a little variation in the extracted charge carrier mobility for the devices fabricated under similar experimental conditions, therefore, multiple OFETs were fabricated under each condition in order to study the statistical distributions. This difference in the inter-device performances might also be

originated from the variations in the octadecyltrichlorosilane (OTS) surface treatment of SiO_2 insulator,[48,49] since the charge transport in FET typically occurs at the semi-conductor/insulator interface which plays a dominant role in controlling the carrier transport especially in case of pBTTT.[25,45,50] A p-type charge transport can be clearly seen in the OFETs, however, high output currents were observed in the OFETs when channel direction was || compared to that with ⊥ at the same gate bias voltage. The average FET mobility measured with channel || to orientation direction was found to be 0.4 $cm^2V^{-1}s^{-1}$ with maximum mobility of 1.24 $cm^2V^{-1}s^{-1}$ while it was 0.04 $cm^2V^{-1}s^{-1}$ (Maximum 0.05 $cm^2V^{-1}s^{-1}$) for the ⊥ orientation. All of the devices typically had considerably high on/off ratio in the range 10^6 to 10^7. It is worth to mention here that when the same material was spin-coated with identical OTS treated SiO_2 substrate, the mobility was considerably low (0.07 $cm^2V^{-1}s^{-1}$-0.09 $cm^2V^{-1}s^{-1}$) (supporting information Figure S3). The observed saturation field effect mobility in parallel direction is one of the highest amongst the reported values of mobility for this class of material (pBTTT). It should be noted that such a high performance demonstrated by other groups was only achieved by employing high work function metal (platinum) source and drain electrodes and decreasing channel length of 5 μm to decrease the contact resistance at metal/semiconductor interface.[51] Generally the transport anisotropy in oriented thiophene based polymer films depends on the orientation of majority crystallite edge-on/face- on and orientation intensity of the polymer backbone. Edge-on favors low transport anisotropy and face-on orientation offers high transport anisotropy, on the other side high orientation favors high transport anisotropy. XRD results for the oriented films of pBTTT processed by FTM as discussed above shows that these crystallites in oriented film exhibited ideal edge-on orientations without any face-on fractions.

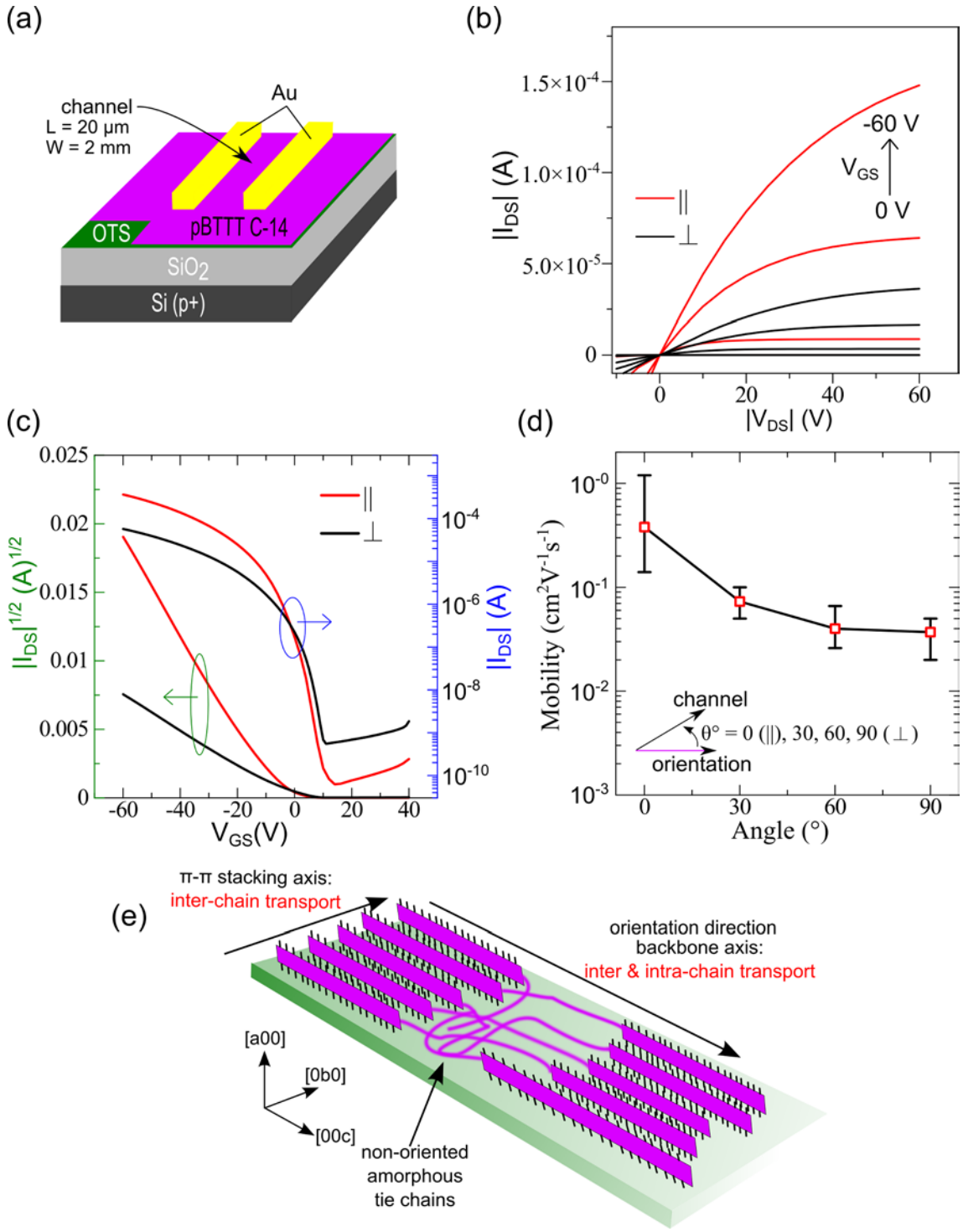

Figure 5. (a) Schematic device architecture of the fabricated OFET, Output (b) and transfer characteristics (c) parallel (||) and perpendicular (⊥) to the orientation direction of the pBTTT, (d) Variation of field effect mobility at different angles with respect to the orientation direction and (e) schematic illustration showing the possible charge transport in edge-on oriented crystallite. Transfer characteristics were taken with V_{DS} = -80 V and the average field effect mobility were estimated by taking the average of at least 6 to 10 devices.

A similar kind of opto-electronic anisotropies have also been reported for the edge-on oriented pBTTT films with DR=6.5 and $\mu_{\parallel}/\mu_{\perp}$~ 3-5 by Lee et al.,[25] and DR=13 with $\mu_{\parallel}/\mu_{\perp}$~ 10 by Biniek et al. under similar device configurations.[26] Where as in our case the edge-on oriented films with DR~13 exhibited $\mu_{\parallel}/\mu_{\perp}$~ 10, higher than Lee et al. whose thin films were prepared by heating the films above the second LC phase transition temperature (>250^{o}C) related to the melting of polymer backbones (ribbon phase) to induce oriented ribbon phase with edge-on crystallites.[25] Therefore, in the present case for OFET based on FTM processed pBTTT, observation of such a high charge carrier mobility along the backbone direction is credited its origin from the highly aligned polymeric backbones. In general the origin of the anisotropy in mobility arises not only from the orientation of the crystallites but also the orientation intensity. Previously, Hosokawa et al. have already demonstrated that with in the same thiophene having the same intensity of orientation, edge-on oriented films exhibited less anisotropy (~1 order) as compared to that of its face-on (~2-3 order) counterparts.[52] In order to precisely elucidate the role of molecular orientation and π-π stacking on field effect mobility, orientation direction of the polymer was varied at different angles with respect to the channel direction as shown in Figure 5d. To avoid any kind of variations originating from device to device variation, efforts were also made to analyze the variation with in the same OFET substrates by fabricating the multiple devices. A perusal of this figure clearly corroborates that there is a sharp decrease in average field effect mobility and significant drops of ~5 times, ~9 times and ~10 times when the polymer orientation direction was at 30°, 60°, 90° with respect to channel direction, respectively. These results suggest that charge carrier mobility along the backbone direction (0°) dominates due the orientation of the majority of the polymer main chains and some randomly aligned polymers (tie-chains) acting as transport bridge to connect the crystalline domains as schematically illustrated in (Figure 5e). On the other hand, when measured at other angles the transport capability depends on π-π

stacking, which plays an important role in controlling the carrier transport. Therefore, it can be concluded that the charge transport along the π-π stacking direction exhibits ~1 order less as compared to main chain direction. It should be noted that we have not optimized the device fabrication conditions in terms of decreasing the interfacial roughness of the dielectric,[43] precise surface treatment,[50,53] molecular weights/polydispersity index,[54] decreased channel length,[51] use of high work function electrodes.[51] Moreover, all of the OFETs were fabricated under ambient conditions using commercial pBTTT C14 without any prior purification leaving still a room for further improvement. This possibility is further being strengthened considering the fact that when pBTTT C-14 was spin-coated in our case exhibited diminished average mobility (0.07 $cm^2V^{-1}s^{-1}$-0.09 $cm^2V^{-1}s^{-1}$) which has been reported to be rather high when fabricated under optimized (0.2 $cm^2V^{-1}s^{-1}$-0.4 $cm^2V^{-1}s^{-1}$) reported by other groups.[25,43]

3. Conclusions

FTM has been successfully utilized to prepare highly oriented and large scale thin films of pBTTT and use of such films led to anisotropic charge carrier transport and enhanced field effect mobilities along the orientation direction. The anisotropic electrical characteristics are advantageous in circuit design especially to isolate neighboring components without requiring a large spatial separation or patterning of the active semiconductor layer. Annealing of the oriented FTM films fabricated under ambient conditions resulted in to an optical anisotropy of 13 as confirmed by polarized electronic absorption spectrum. A combination of out of plane and in-plane X-ray diffractograms it has been demonstrated that polymeric chains in the FTM processed thin films are highly oriented with preferred edge on orientation. This optical anisotropy has been well translated in to electrical characteristics where there was more than an order of magnitude increase in the

charge carrier mobility when direction of the orientation was parallel to the channel direction as compared to that of its perpendicular orientation counterparts. We believe that further optimization of parameters like gate dielectrics, surface treatment, channel length and high work-function electrodes etc. in OTFT devices are expected to result in to even superior anisotropic electrical characteristics.

4. Experimental Section

Materials and Thin Film Preparation: pBTTT were purchased from Sigma Aldrich and used without further purification. Dehydrated chloroform, 1, 2 dichlorobenzene were purchased from the Wako Chemicals and Sigma Aldrich. 1 weight % solution of the pBTTT was prepared in the hot dehydrated chloroform. For preparation of floating films by FTM, about 15 µl of solutions were dropped in the center of the petri-dish containing EG and GL having ratio 3:1 at 55°C and floating films were stamped on the required substrates for characterization. Spin-coated samples were prepared in the mixture of chloroform/1,2 dichlorobenzene (1:1) according to the thickness requirement from the 0.25 weight % solution for OFETs and 2.5 weight % for XRD samples. Normal glass slides shown in Figure 2 were used for all of the characterization pertaining to the POM imaging, electronic absorption spectroscopy and Raman spectroscopy. All the samples were annealed in argon atmosphere at 180°C for 2 minutes and remained on it to slowly cool down to room temperature.

Film Characterization: POM images were obtained using Olympus BX51 polarizing optical microscope (Olympus, Tokyo, Japan). All of the textures were obtained at room temperature. The images were obtained by rotating cross polarizer from 00º to 90º. UV-visible electronic absorption spectrum was measured using UV-Vis-NIR spectrophotometer (JASCO V-570). For polarized absorption spectra, Glan-Thomson Prism was added between the source and detector. Polarized Raman Spectroscopy was carried out by Horiba Jobin Yvon T6400 Micro Raman using a He–Ne Laser operating at $\lambda = 632.8$ nm. The laser power at 1.8 mW was kept constant throughout measurements. Spectral data were obtained at an optical resolution of 50× objective lens and exposure time 5 sec with 3 accumulations to obtain data with a sufficiently high signal-to-noise ratio. The sample stage was rotated against polarization direction of the incident beam and Raman spectra were recorded at every 30º between 00º to 90º. AFM measurements were carried out with JEOL SPM 5200 having probes of Olympus

(OMCL-AC200TS-C3) to investigate the surface topography under tapping mode of the same OFET devices near the channel area. Out-of-Plane X-ray diffraction measurements were carried out with Rigaku X-ray diffractometer having Cu Kα radiations operating at 40 KV and 20 mA. For in-plane GIXD, Rigaku smart lab was used. The in-plane incident angle was kept above the critical angle of the substrate and measurement was performed both along the polymer orientation direction as well as perpendicular to the orientation as reported earlier.[55]

Device Fabrication and Characterization: OFETs were fabricated in the bottom gate top contact device architecture. Oriented film was transferred by stamping on highly doped silicon substrates having SiO_2 (300 nm) as gate dielectric with capacitance (C) of 10 nF. The SiO_2 surface was treated to have the self-assembled monolayer of octadecyltrichlorosilane (OTS). The substrates were immersed in 10 mM solution of OTS in the octadecene in a closed glass bottle at 100°C for 3 hours followed by washing in mixture of super dehydrated chloroform: cyclohexane for 10 mins in ultrasonic bath and dried at 100°C for 1 hour. Oriented floating films were annealed as discussed previously. Gold was thermally evaporated at a pressure of 10^{-6} Torr to form the source and drain electrodes with a nickel shadow mask. The channel length (L) and width (W) was 20 μm and 2 mm, respectively. Devices were exposed in air and output and transfer characteristics were measured with computer controlled two channel source meter Keithley source-meter. Field-effect mobilities were determined from the transfer curve in the saturation region.

Supporting Information

Supporting Information is available from the Wiley Online Library or from the author.

Acknowledgements

This work was financially supported by JSPS Grant-in-Aid for Scientific Research (c) (Grant Number 15K05989). Authors are thankful to Mr. Keisuke Michiki from instrumentation center of Kitakyushu University for his assistance in the X-ray diffraction measurements.

Received: ((will be filled in by the editorial staff))
Revised: ((will be filled in by the editorial staff))
Published online: ((will be filled in by the editorial staff))

References

[1] S. R. Forrest, *Nature* **2004**, *428*, 911.

[2] H. Sirringhaus, *Adv. Mater.* **2014**, *26*, 1319.

[3] A. L. Briseno, R. J. Tseng, M. M. Ling, E. H. L. Falcao, Y. Yang, F. Wudl, Z. Bao, *Adv. Mater.* **2006**, *18*, 2320.

[4] A. L. Briseno, J. Aizenberg, Y. J. Han, R. A. Penkala, H. Moon, A. J. Lovinger, C. Kloc, Z. Bao, *J. Am. Chem. Soc.* **2005**, *127*, 12164.

[5] I. Mcculloch, M. Heeney, M. L. Chabinyc, D. Delongchamp, R. J. Kline, M. C??lle, W. Duffy, D. Fischer, D. Gundlach, B. Hamadani, R. Hamilton, L. Richter, A. Salleo, M. Shkunov, D. Sparrowe, S. Tierney, W. Zhang, *Adv. Mater.* **2009**, *21*, 1091.

[6] L. Janasz, D. Chlebosz, M. Gradzka, W. Zajaczkowski, T. Marszalek, K. Müllen, J. Ulanski, A. Kiersnowski, W. Pisula, *J. Mater. Chem. C* **2016**, *4*, 11488.

[7] N. E. Persson, P.-H. Chu, M. McBride, M. Grover, E. Reichmanis, *Acc. Chem. Res.* **2017**, *50*, 932.

[8] M. Pandey, S. Nagamatsu, S. S. Pandey, S. Hayase, W. Takashima, *Org. Electron.* **2016**, *38*, 115.

[9] E. J. W. Crossland, K. Tremel, F. Fischer, K. Rahimi, G. Reiter, U. Steiner, S. Ludwigs, *Adv. Mater.* **2012**, *24*, 839.

[10] M. Brinkmann, L. Hartmann, L. Biniek, K. Tremel, N. Kayunkid, *Macromol. Rapid Commun.* **2014**, *35*, 9.

[11] Y. Yao, H. Dong, W. Hu, *Polym. Chem.* **2013**, *4*, 5197.

[12] H. Sirringhaus, P. J. Brown, R. H. Friend, M. M. Nielsen, K. Bechgaard, B. M. W. Langeveld-Voss, a. J. H. Spiering, R. a. J. Janssen, E. W. Meijer, P. Herwig, D. M. de Leeuw, *Nature* **1999**, *401*, 685.

[13] J. F. Chang, B. Sun, D. W. Breiby, M. M. Nielsen, T. I. Sölling, M. Giles, I.

McCulloch, H. Sirringhaus, *Chem. Mater.* **2004**, *16*, 4772.

[14] H. Yang, S. W. Lefevre, C. Y. Ryu, Z. Bao, *Appl. Phys. Lett.* **2007**, *90*, 1.

[15] S. Nagamatsu, W. Takashima, K. Kaneto, Y. Yoshida, N. Tanigaki, K. Yase, K. Omote, *Macromolecules* **2003**, *36*, 5252.

[16] M. Misaki, Y. Ueda, S. Nagamatsu, Y. Yoshida, N. Tanigaki, K. Yase, *Macromolecules* **2004**, *37*, 6926.

[17] L. Hartmann, K. Tremel, S. Uttiya, E. Crossland, S. Ludwigs, N. Kayunkid, C. Vergnat, M. Brinkmann, *Adv. Funct. Mater.* **2011**, *21*, 4047.

[18] B. O'Connor, R. J. Kline, B. R. Conrad, L. J. Richter, D. Gundlach, M. F. Toney, D. M. DeLongchamp, *Adv. Funct. Mater.* **2011**, *21*, 3697.

[19] X. Xue, G. Chandler, X. Zhang, R. J. Kline, Z. Fei, M. Heeney, P. J. Diemer, O. D. Jurchescu, B. T. O'connor, *ACS Appl. Mater. Interfaces* **2015**, *7*, 26726.

[20] B. O'Connor, E. P. Chan, C. Chan, B. R. Conrad, L. J. Richter, R. J. Kline, M. Heeney, I. McCulloch, C. L. Soles, D. M. DeLongchamp, *ACS Nano* **2010**, *4*, 7538.

[21] T. Morita, V. Singh, S. Nagamatsu, S. Oku, W. Takashima, K. Kaneto, *Appl. Phys. Express* **2009**, *2*, 1.

[22] J. Noh, S. Jeong, J.-Y. Lee, *Nat. Commun.* **2016**, *7*, 12374.

[23] M. Pandey, S. S. Pandey, S. Nagamatsu, S. Hayase, W. Takashima, *J. Nanosci. Nanotechnol.* **2017**, *17*, 1915.

[24] I. McCulloch, M. Heeney, C. Bailey, K. Genevicius, I. Macdonald, M. Shkunov, D. Sparrowe, S. Tierney, R. Wagner, W. Zhang, M. L. Chabinyc, R. J. Kline, M. D. McGehee, M. F. Toney, *Nat. Mater.* **2006**, *5*, 328.

[25] M. J. Lee, D. Gupta, N. Zhao, M. Heeney, I. Mcculloch, H. Sirringhaus, *Adv. Funct. Mater.* **2011**, *21*, 932.

[26] L. Biniek, N. Leclerc, T. Heiser, R. Bechara, M. Brinkmann, *Macromolecules* **2013**, *46*, 4014.

[27] Z. Zheng, K. H. Yim, M. S. M. Saifullah, M. E. Welland, R. H. Friend, J. S. Kim, W. T. S. Huck, *Nano Lett.* **2007**, *7*, 987.

[28] N. I. C. Alignment, H. T. N. Defined, N. Lithography, *ACS Nano* **2009**, *3*, 3085.

[29] H. Sirringhaus, R. J. Wilson, R. H. Friend, M. Inbasekaran, W. Wu, E. P. Woo, M. Grell, D. D. C. Bradley, *Appl Phys Lett* **2000**, *77*, 406.

[30] A. Kumar, W. Takashima, K. Kaneto, R. Prakash, *J. Appl. Polym. Sci.* **2014**, *131*.

[31] M. K. Singh, A. Kumar, R. Prakash, *Mater. Sci. Eng. B* **2017**, *217*, 12.

[32] D. M. Delongchamp, R. J. Kline, Y. Jung, D. S. Germack, E. K. Lin, A. J. Moad, L. J. Richter, M. F. Toney, M. Heeney, I. Mcculloch, *ACS Nano* **2009**, *3*, 780.

[33] R. K. Pandey, A. K. Singh, R. Prakash, *J. Phys. Chem. C* **2014**, *118*, 22943.

[34] M. S. Park, A. Aiyar, J. O. Park, E. Reichmanis, M. Srinivasarao, *J. Am. Chem. Soc.* **2011**, *133*, 7244.

[35] A. Hamidi-Sakr, L. Biniek, S. Fall, M. Brinkmann, *Adv. Funct. Mater.* **2016**, *26*, 408.

[36] T. Higashi, N. Yamasaki, H. Utsumi, H. Yoshida, A. Fujii, M. Ozaki, *Appl. Phys. Express* **2011**, *4*, 91602.

[37] J. Soeda, H. Matsui, T. Okamoto, I. Osaka, K. Takimiya, J. Takeya, *Adv. Mater.* **2014**, *26*, 6430.

[38] P. Brown, D. Thomas, A. Köhler, J. Wilson, J.-S. Kim, C. Ramsdale, H. Sirringhaus, R. Friend, *Phys. Rev. B* **2003**, *67*, 1.

[39] M. L. Chabinyc, M. F. Toney, R. J. Kline, I. McCulloch, M. Heeney, *J. Am. Chem. Soc.* **2007**, *129*, 3226.

[40] T. Schuettfort, B. Watts, L. Thomsen, M. Lee, H. Sirringhaus, C. R. McNeill, *ACS Nano* **2012**, *6*, 1849.

[41] J. Gao, A. K. Thomas, R. Johnson, H. Guo, J. K. Grey, *Chem. Mater.* **2014**, *26*, 4395.

[42] S. Qu, Q. Yao, L. Wang, Z. Chen, K. Xu, H. Zeng, W. Shi, T. Zhang, C. Uher, L. Chen, *NPG Asia Mater.* **2016**, *8*, e292.

[43] Y. Jung, R. Joseph Kline, D. A. Fischer, R. J. Kline, M. Heeney, L. McCulloch, D. M. DeLongchamp, *Adv. Funct. Mater.* **2008**, *18*, 742.

[44] M. Pandey, S. S. Pandey, S. Nagamatsu, S. Hayase, W. Takashima, *Thin Solid Films* **2016**, *619*, 125.

[45] R. J. Kline, D. M. DeLongchamp, D. A. Fischer, E. K. Lin, L. J. Richter, M. L. Chabinyc, M. F. Toney, M. Heeney, I. McCulloch, *Macromolecules* **2007**, *40*, 7960.

[46] M. L. Chabinyc, *Polym. Rev.* **2008**, *48*, 463.

[47] L. H. Jimison, M. F. Toney, I. McCulloch, M. Heeney, A. Salleo, *Adv. Mater.* **2009**, *21*, 1568.

[48] A. Salleo, M. L. Chabinyc, M. S. Yang, R. A. Street, *Appl. Phys. Lett.* **2002**, *81*, 4383.

[49] T. Kushida, T. Nagase, H. Naito, *Appl. Phys. Lett.* **2014**, *104*.

[50] T. Umeda, D. Kumaki, S. Tokito, *J. Appl. Phys.* **2009**, *105*.

[51] B. H. Hamadani, D. J. Gundlach, I. McCulloch, M. Heeney, *Appl. Phys. Lett.* **2007**, *91*, 1.

[52] Y. Hosokawa, M. Misaki, S. Yamamoto, M. Torii, K. Ishida, Y. Ueda, *Appl. Phys. Lett.* **2012**, *100*, 203305.

[53] T. Umeda, S. Tokito, D. Kumaki, *J. Appl. Phys.* **2007**, *101*, 54517.

[54] A. Gasperini, K. Sivula, *Macromolecules* **2013**, *46*, 9349.

[55] S. Nagamatsu, M. Misaki, M. Chikamatsu, T. Kimura, Y. Yoshida, R. Azumi, N. Tanigaki, K. Yase, *J. Phys. Chem. B* **2007**, *111*, 4349.

Table of Content

Directed and rapid self-assembly leading to macroscopically oriented floating films of high mobility thienothiophene has been prepared by newly developed FTM method. Oriented films are highly crystalline with preferred edge-on orienation. These films exhibit high optical and electrical anisotropy along with pronounced field effect mobility reaching 1.24 $cm^2/V.s$ along the orientation direction.

Keyword:

Self-assembly, Orientation, Thienothiophene, Anisotropic-transport, OFET

Manish Pandey, Ashwathanarayana Gowda, Shuichi Nagamatsu, Sandeep Kumar, Wataru Takashima, Shuzi Hayase and Shyam S. Pandey**

Title

Rapid formation of Macroscopic Self-Assembly of Liquid Crystalline, High Mobility, Semi-conducting Thienothiophene

ToC Figure

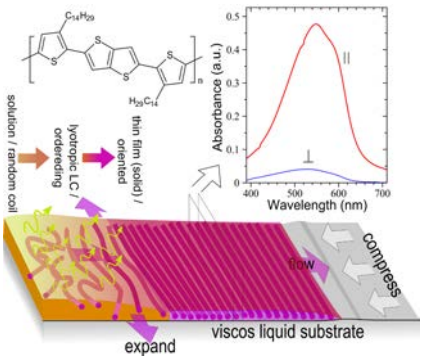

Supporting Information

Rapid formation of Macroscopic Self-Assembly of Liquid Crystalline, High Mobility, Semi-conducting Thienothiophene

Manish Pandey*, Ashwathanarayana Gowda, Shuichi Nagamatsu, Sandeep Kumar, Wataru Takashima, Shuzi Hayase and Shyam S. Pandey*

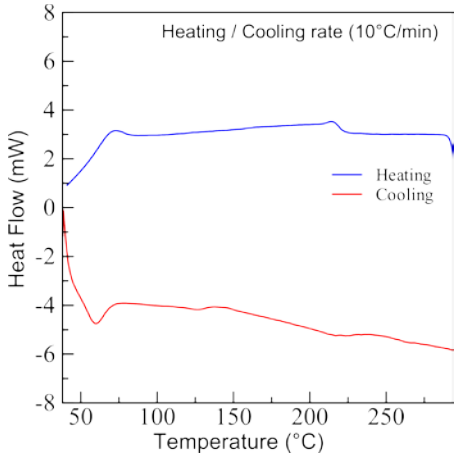

Figure S1. Differential scanning calorimeter measurement of pBTTT c-14

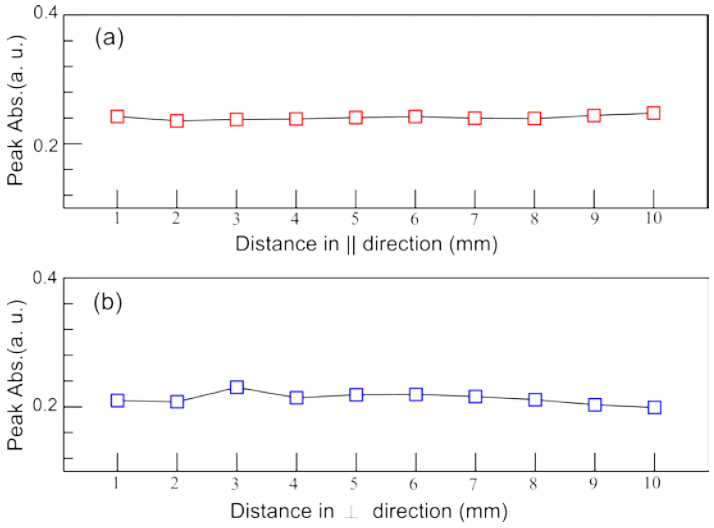

Figure S2. Variation of peak absorption intensity across 1 cm in the oriented film casted on glass slide, (a) along the orientation direction (||) and (b) perpendicular to it.

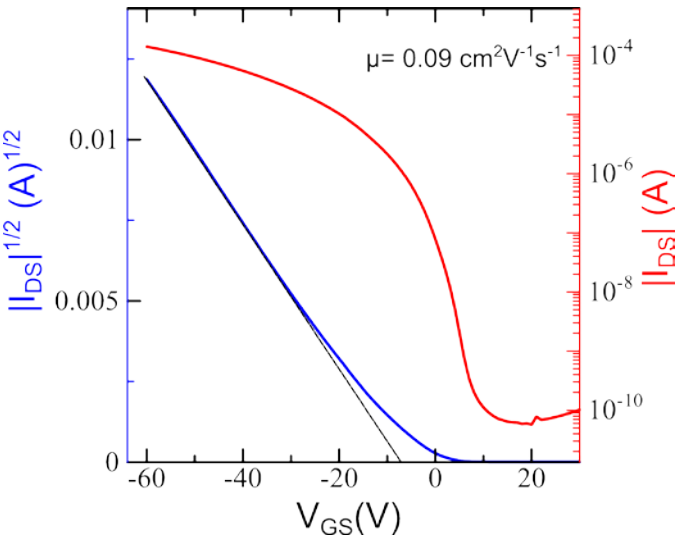

Figure S3. Transfer curve of Spin-coated pBTTT c-14 (V_{DS} = -100 V).

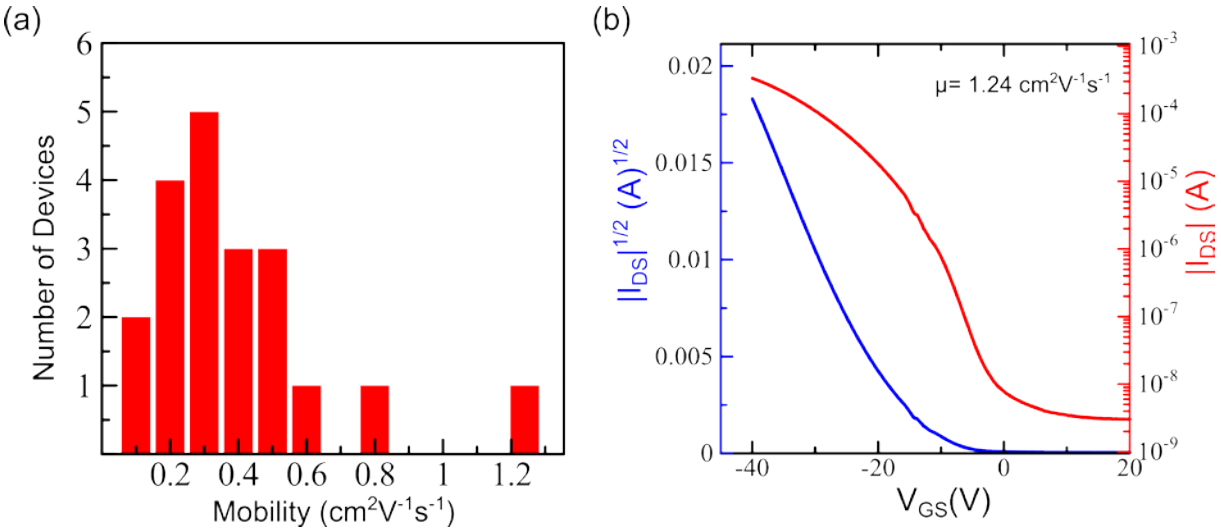

Figure S4. (a) Histogram of the mobility in the devices with channel parallel to orientation direction of pBTTT C-14 and (b) Transfer curve of the highest device exhibited highest mobility (V_{DS}=-100V).